

Static versus dynamic friction: The role of coherence

Zeno Farkasy, S lvio R. Dahmen^z and D. E. Wolf^y

^y Department of Physics, Universitat Duisburg-Essen, D -47048 Duisburg, Germany and

^z Instituto de Física da UFRGS, CP 15051, 90501-970 Porto Alegre RS, Brazil

A simple model for solid friction is analyzed. It is based on tangential springs representing interlocked asperities of the surfaces in contact. Each spring is given a maximal strain according to a probability distribution. At their maximal strain the springs break irreversibly. Initially all springs are assumed to have zero strain, because at static contact local elastic stresses are expected to relax. Relative tangential motion of the two solids leads to a loss of coherence of the initial state: The springs get out of phase due to differences in their sizes. This mechanism alone is shown to lead to a difference between static and dynamic friction forces already. We find that in this case the ratio of the static and dynamic coefficients decreases with increasing relative width of the probability distribution, and has a lower bound of 1 and an upper bound of 2.

While the facts that dry solid friction is proportional to the normal load at the contact and does not depend on the apparent contact area were established experimentally at least as early as in the 16th century by Leonardo da Vinci and are now known under the names of Amontons (1699) or Coulomb (1781) [1], it was probably Euler (1750) who first distinguished between static and dynamic friction [2]. This difference has been explained in several, conceptually different ways. The reason was identified as: A collective depinning phenomenon [3], the time strengthening of individual pinning sites [4, 5], the shear melting of a lubrication film [6], mobile impurities at the interface [7], or the formation and healing of microcracks [8]. The fact that all these mechanisms lead to the same macroscopic phenomenology raises the question whether they can be classified in terms of more abstract concepts.

An attempt in this direction was made by Caroli and Nozières [9], who proposed a model for dry solid friction based on the following physical picture: The surfaces have randomly distributed asperities which get interlocked. These interlocked asperities act as pinning sites resisting tangential motion. Under tangential load they are deformed up to a threshold

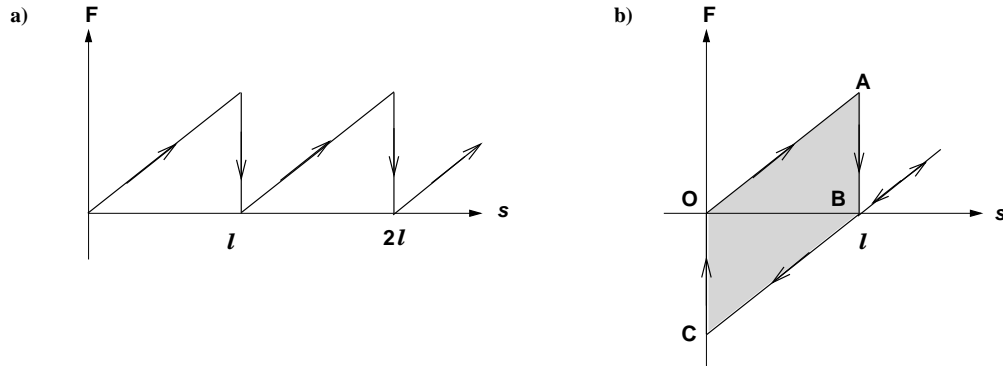


FIG. 1: a) Schematic plot of the force F as a function of displacement s is presented. At the threshold l the spring breaks and immediately reattaches. b) By reversing the displacement the force also changes sign. During the complete cycle $O \rightarrow A \rightarrow B \rightarrow C \rightarrow O$ energy is dissipated irreversibly and is numerically equal to the shaded area. The size of the hysteresis loop is proportional to the threshold length l .

(which these authors call "spinodal limit"), where they break irreversibly releasing their energy in the form of phonons into the bulk. The threshold is a measure for the pinning strength. They argue that their model does not lead to a difference between static and dynamic friction, unless the strain of the pinning sites has different statistics in the static and in the sliding case or aging is taken into account. The latter aspect has been further investigated in ref. [5] and explains also the experimentally observed time strengthening and velocity weakening of the pinning sites.

However, time strengthening is a slow process. This motivates us to explore in more detail what would be the influence of strain statistics at the pinning sites on the static and dynamic friction coefficients, μ_s and μ_d . Although time strengthening will not be considered, it can be included in addition to account for, e.g., velocity weakening.

The model we consider in the following captures, we believe, the essence of the physical picture described above and at the same time highlights the concept of coherence, which is an ingredient in several different models (see [10] and references therein). For the sake of clarity and analytical tractability we work out only a one-dimensional version, but the extension to the two-dimensional case is straightforward.

Consider two solid bodies in contact, one being the fixed substrate (the "track") and the other the body to be displaced (the "slider"). To keep the equations simple, we consider

only motion in a fixed direction. Reversing the direction would lead to hysteretic behaviour like in Fig. 1. The friction force arises from interlocked asperities in the contact area, which are modelled here by linear springs with zero equilibrium length (see also [11]), which only act in the tangential direction. Each spring has one end attached to the slider, while the other end is attached to the track. When the slider moves, each spring gets stretched up to an individual threshold length ℓ , where it breaks. The elastic energy stored in a spring is completely dissipated when it breaks.

In contrast to previous work [11] we take here explicitly into account that the interlocked asperities are characterized by different threshold lengths ℓ with a probability distribution $p(\ell)$, normalized as $\int_0^{R_1} p(\ell) d\ell = 1$. There is experimental evidence that this distribution is approximately Gaussian centered around a characteristic length [12].

In general the number of pinning sites and the distribution of their strength $p(\ell)$ will change with time during a transient until steady state sliding is reached. However, one can imagine experimental situations where both are time independent, at least in an average sense [13]. Here we make this assumption deliberately in order to show that a difference between static and dynamic friction can ensue, even if the number of pinning sites and the distribution of their strength are time independent. With this assumption a new spring with the same parameter ℓ has to become active whenever one breaks. Hence the elastic restoring force from springs of threshold length ℓ becomes simply a sawtooth-like function of the displacement s (see Fig. 1). This displacement is assumed to be the same for all springs (approximation of a rigid slider). The friction force is the sum of all these elastic restoring forces. In the following all spring constants k are assumed to be the same, but this is not crucial. For example we checked that spring constants proportional to ℓ give qualitatively the same results.

The crucial ingredient of our model will be discussed now. During sliding all springs will be stretched in the sliding direction by a random fraction of their threshold lengths. When the motion is stopped, the slider will recoil so that some springs get stretched in the opposite direction until the net force on the slider is zero (in the absence of an external shear force). In contrast to [9] we assume here that then the strain distribution becomes narrower, because the springs have time to relax. We have to discard plastic flow as the main relaxation mechanism when relative motion comes to a halt, since the speed of this process is proportional to the difference between applied stress and yield stress and should be therefore

too slow. A different mechanism is required, which is slow compared to the lifetime τ_v of stretched springs during sliding with velocity v , but fast compared to the time a stationary contact is at rest. One possibility might be viscoelasticity: During sliding a nonequilibrium density of point defects in the immediate neighborhood of the surface is created. These point defects can be viewed as a viscous fluid penetrating the crystal lattice: if the lattice is exposed to time dependent stresses at very high frequencies during sliding, the defects hardly have time to diffuse and contribute to stress relaxation. However, if the frequency is low or even zero, as in the static case, the point defects move due to thermal activation to regions where they reduce the elastic energy of the entangled asperities (we note that this is different from plastic flow, which is due to the motion of dislocations). Diffusion of point defects is also a slow process, but since the distances are at the nm to μ m scale, and since it may be assisted by strain, which can considerably reduce activation energies, it is still faster than plastic deformation. Consequently we expect that microscopic interface strains relax relatively fast in the static, but not fast enough in the sliding case. Conceptually this is different from time strengthening, where atomic diffusion would shift the threshold lengths ℓ^* towards larger values, an effect that occurs in addition, but is neglected here for the sake of working out the effect of strain coherence more clearly.

In the context of our model we actually consider the extreme case, where all springs relax to zero elastic energy, as soon as sliding stops (full "coherence"). With the assumption that all springs are relaxed initially, the friction force as a function of displacements for an apparent (macroscopic) contact area A and the number density n_p of active pinning sites (or springs) reads

$$f(s) = A n_p k \int_0^{\ell^*} p(\varphi) t(\varphi; s) d\varphi; \quad (1)$$

where $t(\varphi; s) = s \bmod \ell^*$ is a sawtooth-shaped function of periodicity ℓ^* . The phase of this periodic function is $\varphi(\varphi; s) = t(\varphi; s)/\ell^*$, which is a number between 0 and 1. The behaviour of eq. (1) is closely related to the probability distributions of these phases,

$$w(\varphi; s) = \int_0^{\ell^*} p(\varphi) \frac{t(\varphi; s)}{\ell^*} d\varphi; \quad (2)$$

For example $w(0; s)$ is the probability density of springs that break at displacement s . As these springs still contribute their elastic restoring force to $f(s - ds/2)$ but no longer to

$f(s + ds=2)$, the derivative of eq. (1) is given by

$$f^0(s) = A n_p k [1 - w(0;s)] : \quad (3)$$

This can be derived from eq. (1) using the expression (5) given below.

Whereas the initial state is coherent in the sense that $w(0;0) = 1$, coherence gets lost for large displacement, where all phases become equally likely:

$$\lim_{s \rightarrow \infty} w(0;s) = 1 : \quad (4)$$

To prove this we evaluate the integral in eq. (2) around each of the discrete values of φ for which the argument of the δ -function vanishes and obtain

$$w(0;s) = \sum_{m=1}^{\infty} p\left(\frac{s}{m+1}\right) \frac{s}{(m+1)^2} : \quad (5)$$

Introducing the variable $x = (m+1)s$, which becomes quasi-continuous for large s , this converges to the Riemann-integral (provided $p(\varphi)$ is a Riemann-integrable function)

$$\lim_{s \rightarrow \infty} w(0;s) = \int_0^{\infty} p\left(\frac{1}{x}\right) \frac{1}{x^2} dx = \int_0^{\infty} p(y) dy = 1 ; \quad (6)$$

where the variable transformation $y = 1/x$ was used, and the last equality is just the normalization of the distribution. This shows that after sufficient displacement the system forgets its initially coherent state. An important consequence of this decoherence is that the friction force for large displacements becomes constant. This follows immediately from eq. (3), because w tends to 1. Then the value of the friction force in eq. (1) coincides with its average,

$$\langle f \rangle = A n_p \frac{k}{2} \int_0^{\infty} p(\varphi) \varphi d\varphi = A n_p \frac{k}{2} \langle \varphi \rangle ; \quad (7)$$

where $\langle \varphi \rangle$ is the average maximum spring length.

Figure 2a shows the friction force $f(s)$ as a function of displacement s on a microscopic length scale, for three different distributions $p(\varphi)$. For the numerical evaluation it was useful to rewrite the force $f(s)$ in eq. (1) by integrating eq. (3), after formula (5) has been inserted:

$$f(s) = A n_p k \int_0^s \sum_{m=1}^{\infty} p\left(\frac{s}{m+1}\right) \frac{s}{(m+1)^2} ds : \quad (8)$$

In this expression the integrals can be calculated analytically for simple distributions, e.g., truncated Gaussians. All curves in fig. 2a have in common that they start from zero with

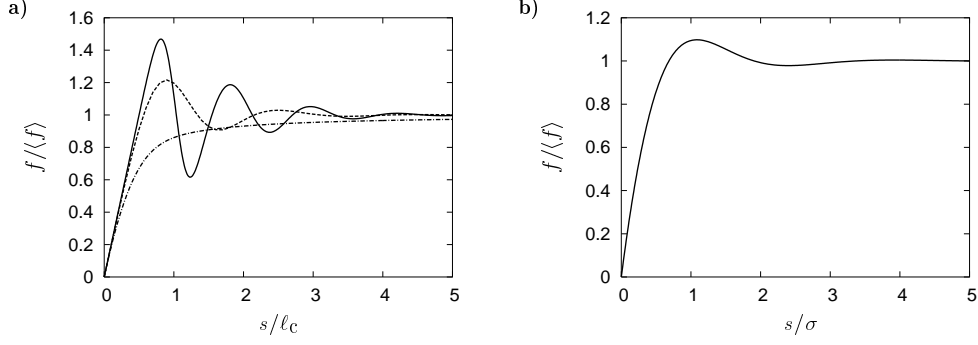


FIG. 2: a) Friction force f as a function of displacement s of the slider for different maximum spring length distributions $p(\ell)$. $\langle f \rangle$ is the dynamic friction force, ℓ_c is a characteristic maximum spring length. Solid line for a truncated Gaussian distribution, $p(\ell) / \exp[-(\ell - \ell_c)^2/2(\sigma)^2]$ with width $\sigma = 0.15 \ell_c$. Dashed line for the same Gaussian distribution, but with width $\sigma = 0.4 \ell_c$. Dashed-dotted line for $p(\ell) / 1 = [1 + (\ell/\ell_c)^3]$, width is $\sigma = \ell_c$. Note that the height of the first peak decreases with increasing width. b) Friction force f as a function of displacement s of the slider for $p(\ell) / \exp[-\ell^2/2(\sigma)^2]$. The maximum value of f is approximately $1.098\langle f \rangle$ at displacement $s = 1.087 \sigma$.

a slope of 2 in the natural units, $\langle f \rangle$ and ℓ_c , and converge to 1 for large displacements. For the truncated Gaussian distributions the force has a maximum at a displacement close to ℓ_c , where a large number of relatively strong springs are just about to break. As long as an external driving force remains smaller than this maximum, the position of the slider will move only on the scale of ℓ_c . Therefore we interpret the first peak of the force as the static friction force, the pulling force needed to initiate motion of the slider. Once the object moves, the force necessary to maintain its motion decays to a smaller value with damped oscillations, which die out again on the scale of ℓ_c . Therefore we interpret the asymptotic force as the dynamic friction force.

We found numerically that the maximum is less pronounced the wider the Gaussian distribution is for a given ℓ_c . This means that the difference between static and dynamic friction decreases. An interesting question is what happens for a distribution with finite average value, but in finite width. An example is shown in Fig. 2a. In this case the force monotonically increases to $\langle f \rangle$, so that according to our interpretation the static and dynamic friction coefficients are equal. However, we regard this example purely as an illustration. As mentioned above, the empirically found distributions are approximately Gaussian.

At this point we can clearly formulate the main message of this paper: In our model the presence of an initial peak of the friction force, meaning that the maximum static friction is larger than the dynamic friction, is the result of an initial coherence in the strain distribution of the interlocked asperities. The height of the peak depends on the distribution of threshold lengths (or loop sizes, see Fig.1). After displacement of the order of few times the average threshold length the initial coherence is forgotten, the strains get out of phase, and as a consequence the friction force decays to the dynamical friction force. While we assume a complete initial coherence in our model, this is not absolutely necessary: Decreasing the level of initial coherence still results in a peak of the friction force, although with a decreased height (results not shown here).

Now we show that the ratio of static and dynamical friction coefficients does not change under a rescaling of loop sizes $\ell \rightarrow a\ell$. With the probability distribution

$$p(\ell) \rightarrow ap(a\ell); \quad (9)$$

one gets according to eq. (1) that the elastic restoring force at displacement s and hence also its maximum value (static friction force) and its average value (dynamical friction force) transform as

$$f(s) \rightarrow \frac{1}{a} f(as); \quad (10)$$

Therefore the ratio between static and dynamic friction remains invariant.

As mentioned above, the probability distribution $p(\ell)$ is approximately Gaussian in many cases [12], i.e. completely characterized by its first and second moments, $\langle \ell \rangle$ and $\langle \ell^2 \rangle$. As under a rescaling $\ell \rightarrow a\ell$ the first and second moments scale differently, $\langle \ell \rangle \rightarrow a\langle \ell \rangle$ and $\langle \ell^2 \rangle \rightarrow a^2\langle \ell^2 \rangle$, but the ratio $\frac{\langle \ell^2 \rangle}{\langle \ell \rangle^2}$ remains invariant, it cannot depend on $\langle \ell \rangle$ and $\langle \ell^2 \rangle$ separately, but only on the invariant combination $\langle \ell^2 \rangle = \langle \ell \rangle^2$:

$$\frac{\langle \ell^2 \rangle}{\langle \ell \rangle^2} = g \left(\frac{\langle \ell^2 \rangle}{\langle \ell \rangle^2} \right); \quad (11)$$

The numerical analysis shows that g is a decreasing function of its argument (this tendency can be seen in Fig. 2a). Therefore the extreme case, where the width of $p(\ell)$ is zero [$p(\ell) =$

$\delta(\ell - \ell_c)$] gives an upper bound on the ratio of the friction coefficients. This case is special, as coherence never gets lost: All springs get stretched up to ℓ_c , break simultaneously and are replaced by fresh, unstrained springs, which again get stretched up to ℓ_c and so forth. (The mathematical reason why our proof that the force converges to the average value is

not valid in this case is that the function is not Riemann-integrable.) Because of the lack of decoherence, the model gives stick-slip motion. However, for dry solid friction this is unphysical: Any small randomness for example of the times, when new interlockings form, would have the effect, that the springs ultimately get out of phase. Then the sawtooth-oscillations of the force $f(s) = A n_p k t(\lambda_c; s)$ would be damped similar to the oscillations shown in fig. 2a and would converge to the average value $\langle f \rangle = A n_p k \lambda_c = 2$, which we still identify with the dynamic friction. Obviously it is half the maximal value of $f(s)$, which we identify with the static friction. This gives an upper bound of 2 for the ratio between the friction coefficients in eq. (11). Note that the upper bound would increase if time strengthening were taken into account.

Together with the lower bound obtained if the relative width of $p(\lambda)$ tends towards infinity, we conclude that the model restricts the ratio of the friction coefficients to the interval

$$1 \leq \frac{\mu_s}{\mu_d} \leq 2 \quad (12)$$

Actually, for Gaussian distributions, a more stringent lower bound, approximately 1.098, can be given. This value is obtained, when the argument of g in eq. (11) tends to infinity, which corresponds to the limit $\lambda = \lambda_c \rightarrow 1$. Then the force $f(s)$ approaches the one obtained for $\lambda_c = 0$, i.e., for $p(\lambda) \propto \exp[-\lambda^2/2]$. For this case the ratio of the friction coefficients is approximately 1.098 (see fig. 2b) independent of λ , due to eq. (10). Lower values can be obtained if $p(\lambda)$ has a power law tail, e.g., $p(\lambda) \propto 1/[\lambda + (\lambda - \lambda_c)^3]$, as shown in fig. 2a.

There is another interesting consequence of this theory. According to the theory of Bowden and Tabor [1], the microscopic contact area of the pinning sites adjusts quickly by plastic flow such that the local stress drops to the yield threshold σ_c of the material. Then the normal load is equal to the real contact area times σ_c :

$$f_n = A n_p \sigma_c h^2 i; \quad (13)$$

where we assumed that a pinning site of loop size λ contributes λ^2 with a constant geometry factor of order 1 to the real contact area. Combining this with eq. (7)

$$f_t = \mu_d f_n = \frac{k}{2} A n_p h^2 i \quad (14)$$

one finds that

$$\frac{\mu_s}{\mu_d} = g \frac{A n_p}{f_n} \frac{k^2}{4 \sigma_c^2} : \quad (15)$$

As the friction coefficients should be independent of f_n , we conclude that the number of pinning sites, $A n_p$, increases proportional to the normal load. This argument is not entirely compelling, as the pinning strength γ needs not be directly related to the microscopic contact area, and also the spring constant k_m might depend on the normal force.

In this work we presented a simple model of dry friction, which explains why static friction force can be larger than dynamic friction force, in terms of the concept of coherence.

Acknowledgments

The authors would like to thank L. Brendel and H. Hinrichsen for fruitful discussions. This work was done within SFB 445 "Nano-particles from the Gas phase: Formation, Structure, Properties".

References

-
- [1] Bowden F P and Tabor D 1958, *The Friction and Lubrication of Solids*, Clarendon Press, Oxford.
 - [2] Duran J 2000, *Sands, Powders, and Grains*, Springer, New York.
 - [3] Volmer A and Nattemann T 1997, *Z. Phys. B* 104, 363.
 - [4] Caroli C and Velicky B 1997, *Friction, Arching, Contact Dynamics*, Eds. Wolf D E and Grassberger P, World Scientific, Singapore, p 13.
 - [5] Caroli C and Velicky B 1997, *J. Phys. I France* 7, 1391.
 - [6] Persson B N J 1996, *Physics of Sliding Friction*, Eds. Persson B N J and Tosatti E, Kluwer Academic Publishers, Dordrecht, p 69.
 - [7] Muser M H, Wenning L and Robbins M O 2001, *Phys. Rev. Lett.* 86, 1295.
 - [8] Gerde E and Marder M 2001, *Nature* 413, 285.
 - [9] Caroli C and Nozieres P 1998, *Eur. Phys. J. B* 4, 233.
 - [10] Muser M H, Urbakh M and Robbins M O 2003, *Adv. Chem. Phys.* 126, 187.
 - [11] Brilliantov N V, Spahn F, Hertzsch J M and Poschel T 1996, *Physica A* 231, 417.

- [12] Greenwood J A 1992, Fundamentals of Friction: Macroscopic and Microscopic Processes, Eds. Singer I L and Pollock H M, Kluwer Academic Publishers, Dordrecht, p. 37.
- [13] Dahmen S R, Farkas Z, Heinrichsen H and Wolf D E 2005, cond-mat 0502293.